Water Resources Research

RESEARCH ARTICLE

10.1029/2017WR022412

Key Points:

- Meteorological drought indices that include evaporation or snowmelt are often strongly correlated with streamflow
- Some of the streamflow records potentially affected by human influences have a weaker correlation with meteorological drought indices
- Drought indices derived from records with a weaker correlation caused by human influences often do not correspond with reported drought impacts

Supporting Information:

- Supporting Information S1

Correspondence to:
E. Tijdeman,
erik.tijdeman@uni-heidelberg.de

Citation:
Tijdeman, E., Barker, L. J., Svoboda, M. D., & Stahl, K. (2018). Natural and human influences on the link between meteorological and hydrological drought indices for a large set of catchments in the contiguous United States. *Water Resources Research*, *54*, 6005–6023. https://doi.org/10.1029/2017WR022412

Received 14 DEC 2017
Accepted 11 JUL 2018
Accepted article online 18 JUL 2018
Published online 5 SEP 2018

Natural and Human Influences on the Link Between Meteorological and Hydrological Drought Indices for a Large Set of Catchments in the Contiguous United States

E. Tijdeman[1], L. J. Barker[2], M. D. Svoboda[3], and K. Stahl[4]

[1]Institute of Geography, Heidelberg University, Heidelberg, Germany, [2]Centre for Ecology and Hydrology, Wallingford, UK, [3]National Drought Mitigation Center, University of Nebraska-Lincoln, Lincoln, NE, USA, [4]Faculty of Environment and Natural Resources, University of Freiburg, Freiburg, Germany

Abstract Precipitation-based drought indices are most commonly used in drought monitoring and early warning systems whereas impacts of drought are often related to other domains of the hydrological cycle such as streamflow. Precipitation droughts do not always coincide with streamflow droughts, as the propagation from precipitation to streamflow is affected by climate, catchment properties, and human influences. For monitoring in ungauged catchments it is the question to what extent drought indices solely based on precipitation or other (more recently developed) meteorological drought indices that include evaporation or snowmelt, have a stronger correlation with streamflow, and whether this correlation is weaker in catchments where streamflow is altered by human influences. Results of a correlation exercise between various meteorological drought indices and streamflow showed that the strongest correlation was often found for meteorological drought indices that include evaporation (especially in drier climates) or snow processes (especially in colder climates). Most catchments with an indicated presence of human influences showed a maximum correlation between meteorological drought indices and streamflow that was comparable in strength to the same correlation for catchments with near-natural flow. However, up to 15% of catchments with an indicated presence of human influences show weaker correlations. Drought indices derived from these influenced records with a weaker correlation do not necessarily correspond to reported drought impacts. In conclusion, knowing which meteorological drought index has the strongest correlation with streamflow in different climate zones has the potential of improving large-scale drought monitoring and early warning systems in ungauged areas or regions that lack real-time streamflow availability.

1. Introduction

Over the past few decades, the U.S. have experienced several major drought events (e.g., Sheffield et al., 2009) that had a negative impact on nature and society (Wilhite et al., 2007). Effective monitoring and early warning of these drought events enabled improved preparedness and resilience (Svoboda et al., 2002). The U.S. Drought Monitor (USDM, http://droughtmonitor.unl.edu/) is one of the few large-scale monitoring products that considers streamflow percentiles within its combined drought index. Elsewhere, the large-scale drought monitoring and early warning systems used for national to multinational identification of regions at risk and policy decisions are more commonly based on meteorological (precipitation-based) drought indicators (Bachmair, Stahl, et al., 2016). However, the impacts of droughts are often caused by deficits in other domains of the hydrological cycle, such as streamflow (Van Lanen et al., 2016), and are thus not directly captured by drought monitoring and early warning systems, which focus on precipitation deficits. Estimating the hydrological drought hazard from precipitation deficits alone has a number of difficulties. The propagation of precipitation deficits through the hydrological cycle is modified by varying climate and catchment controls, as well as human influences, and as such, drought propagation varies between catchments (Van Loon, 2015). Conversely, indices based on hydrological information such as streamflow may not directly or only represent the drought as a natural hazard. As shown and discussed in detail for cases in the UK by Tijdeman et al. (2018), streamflow may show a naturally lagged signal and regulated streamflow may not at all show a drought signal if regulation mitigates the water deficit in the river. Large-scale maps displaying the drought situation based on or including streamflow observations may therefore be less straightforward to interpret regarding the risk of further drought impacts. In the United States, a large number of streamflow records are used routinely, for example, within the USDM or directly by U.S. Geological Survey (USGS) WaterWatch to depict regions at risk from a national or continental point of view. The available information provides an excellent test bed to investigate more generally the link between meteorological and hydrological drought indices and to discuss implications for the role of hydrological information in large-scale monitoring and information portals.

Precipitation and temperature are the main atmospheric drivers of a catchment's water balance and its deficits. Streamflow droughts, defined as below normal streamflow or anomalies (Tallaksen & Van Lanen, 2004), can be initiated by below-normal precipitation and/or below- or above-normal temperatures (Van Loon & Van Lanen, 2012). Above-normal temperatures increase the atmospheric water demand, and consequently can increase the actual evapotranspiration and lower the total water availability and resultant streamflow (e.g., Vicente-Serrano et al., 2014). It was the combination of low precipitation and high temperature (and the subsequent high evapotranspiration) that made the California drought between 2011 and 2014 so severe (Seager et al., 2015). Below-normal temperatures can play a critical role in the time-lag in the propagation of precipitation deficits to streamflow deficits; above-freezing temperatures earlier in the year result in earlier snowmelt and so an earlier streamflow peak. This may result in streamflow droughts later in the year when the snowmelt peak is expected, while below-freezing temperatures that are sustained later than normal can delay the snowmelt peak (Van Loon et al., 2015).

Like temperature, precipitation can follow a seasonal pattern; for example, winters are wetter than summers in the western United States, but are drier in the central United States. Water availability is therefore not constant throughout the year, and the atmospheric demand may be out of phase with the seasonal precipitation signal (Berghuijs et al., 2014). For example, in the western United States, high winter precipitation occurs during periods with relatively low potential evapotranspiration and low summer precipitation coincides with high potential evapotranspiration. In seasonal climates such as these, antecedent conditions are important for water availability in the dry season as shown by the modeling study of Van Loon et al. (2014). If a catchment has already experienced drought at the end of the wet season, there is a low chance of recovery during the dry season. In the case of the 2011–2014 California drought, below-normal winter precipitation led to low snowpack accumulation in the mountains and minimal refilling of the reservoirs, resulting in additional pressures on water supplies later in the year (Seager et al., 2015).

In the absence of human influences, such as reservoir operations or groundwater abstractions, climatological controls have been found to be the dominant control of the streamflow properties (e.g., Berghuijs et al., 2014; Coopersmith et al., 2012). However, catchment characteristics have also been found to modify streamflow, especially during periods of low flow. For example, the propagation from precipitation to streamflow is delayed when precipitation is temporarily stored in lakes, wetlands, or groundwater (e.g., Barker et al., 2016; Peters et al., 2003; Stoelzle et al., 2014). In the presence of human influences, it is questionable whether climate is still the dominant control on the propagation from precipitation to streamflow. Human influences have been associated with both gradual and abrupt changes in low flow magnitude and timing in the eastern United States (Sadri et al., 2016). While it is often possible to generalize the natural controls on streamflow, it can be difficult to generalize the human influences because they can vary in overall impact, timing, and degree. Reservoir operations and groundwater abstractions can both intensify or mitigate the hydrological situation downstream (Tijdeman et al., 2018). Rangecroft et al. (2016) showed a decrease in drought occurrence and severity after the construction of an upstream reservoir used to secure water availability for agriculture downstream. López-Moreno et al. (2009), however, showed an increase in drought occurrence and severity downstream after the construction of a reservoir that stores water during drought. Van Loon and Van Lanen (2013) showed an increase in drought duration and severity compared to the natural situation due to intensive groundwater abstraction whereas Tijdeman et al. (2018) showed an example where groundwater abstractions were likely used to augment streamflow during periods of drought. Other human influences such as diversions, instream abstractions, water transfers, or land use change (e.g., urbanization or intensification or changes in agriculture; e.g., Zhang & Schilling, 2006) also exert a control on streamflow and consequently on the relationship between precipitation and streamflow. Despite these complexities, in a human-modified world, it is critical to account for and understand the human influences on streamflow, especially in densely populated areas where the population may be heavily dependent on surface water for public water supply, agriculture, or industry.

Many drought indices have been developed and applied to characterize meteorological anomalies, for example, the Standardized Precipitation Index (SPI; McKee et al., 1993), the Standardized Precipitation and Evapotranspiration Index (SPEI; Vicente-Serrano et al., 2010; also occasionally used to monitor agricultural droughts), and the Standardized Snow Melt and Rainfall Index (SMRI; Staudinger et al., 2014). These standardized drought indices reflect meteorological anomalies aggregated over different accumulation periods (1, 3, 6, and 12 months are often used). The popularity of meteorological drought indices (especially the SPI; e.g., Bachmair, Stahl, et al., 2016) is partially related to the near-real-time data availability of precipitation as gridded products that cover the entire globe, whereas streamflow measurements are not readily available in many countries in near real-time (Hannah et al., 2011), the United States being one of the exceptions. As the meteorological drought indices only reflect the meteorological drought hazard (and do not necessarily coincide with the total water availability on (or below) the ground, due to various climate/catchment controls and any present human influences), it is important to know which of these factors dominate the propagation of precipitation to streamflow (Van Lanen et al., 2013), and thus which type of meteorological drought index and accumulation period best reflects the hydrological situation.

To improve the understanding of drought propagation, a number of previous studies have assessed the correlation between streamflow and different meteorological drought indices in different regions and climates across the world at different scales, seeking the type of drought index and accumulation period with the highest correlation. The majority of these studies focused on catchments with near-natural flow that are minimally impacted by human influences. For example, higher (summer) correlations between streamflow and the SPEI (compared to the SPI) were found for a set of Austrian and Iberian Peninsula catchments (Haslinger et al., 2014; Vicente-Serrano et al., 2014, respectively) as well as for a set of larger river basins around the globe (Vicente-Serrano et al., 2012). Staudinger et al. (2014) found higher correlations between the SMRI and streamflow (again compared to the SPI) for seven snow influenced Swiss catchments. In catchments with near-natural flow in the UK, stronger correlations were found between longer accumulation periods of the SPI (often >6 months) and streamflow in slow responding, groundwater-fed catchments while streamflow records from fast responding, impermeable catchments showed the highest correlations with short accumulation periods (often <3 months) of the SPI (Barker et al., 2016). Human influences have been shown to decrease the correlation between streamflow and meteorology. Lower correlations were found for the highly influenced basins on the Iberian Peninsula (Vicente-Serrano et al., 2014). For part of the subcatchments of the Ebro basin containing upstream reservoirs, there was an absence of correlation during summer when water levels remain constant in order to fulfill environmental flow requirements and in winter when winter inflows are stored for summer use (López-Moreno et al., 2013).

In this study, we use a similar approach to the one discussed above of comparing the correlation of several meteorological drought indices (SPI, SPEI, and SMRI) with streamflow records for catchments ranging from near-natural to heavily influenced, located within different climatic regimes of the contiguous United States. The objectives of this study are as follows:

1. To analyze the relationship between meteorological and streamflow drought indices under previous studies' hypothesis that the correlation is:
    a. strong in catchments with near-natural flow and;
    b. weaker or absent for some of the catchments with human influences
2. To investigate how meteorological drought indices reflect the streamflow signal depending on the time of year and the climatic setting of the catchment. Hypotheses are the following:
    a. Correlations between streamflow percentiles and the SPEI are strongest in the drier regions, especially in the hotter (summer) months.
    b. Correlations between streamflow percentiles and the SMRI are strongest in mountainous and high-latitude regions, especially in the colder (winter) months.
    c. Correlations between streamflow percentiles and meteorological drought indices in the dry season of climates with seasonality in precipitation are strongest for meteorological drought indices accumulated over long accumulation periods (i.e., that include information about the wet season).

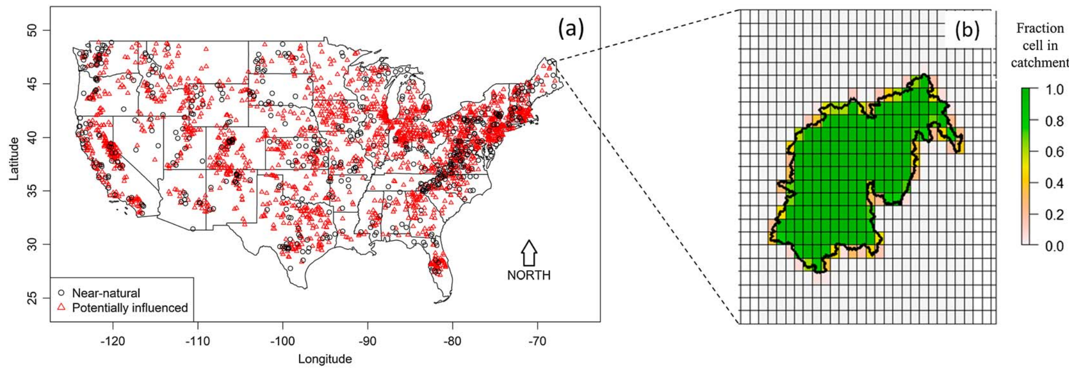

Figure 1. (a) USGS gauging station locations of selected catchments with near-natural streamflow records (black circles) and selected catchments with streamflow records that are potentially influenced by different human influences (red triangles), and (b) example of a catchment boundary (2,252.7 km^2), the underlying PRISM grid (4 km resolution), and the fraction of each PRISM grid cell within the catchment boundaries (indicated by the color).

The first objective aims to elucidate the role of influenced records for use in national to global drought information maps. The second objective aims to generate transferable knowledge to regions with less or less available hydrological information for large-scale drought monitoring. Knowing which meteorological drought index displays the strongest correlation to streamflow in different climatic settings may help to provide surrogate indicators for streamflow in ungauged regions.

In the final step of this study, we investigate the link of streamflow drought indices from catchments with near-natural flow and with potential human influences to the occurrence of reported drought impacts to test how relevant these drought indices are for monitoring the overall impacts of drought. If this is the case, and they are available, direct streamflow measurements would generally be preferable over or at least a very valuable addition to meteorological surrogates.

2. Data and Study Area

The climate of the contiguous United States varies resulting in varying streamflow regimes across the country (e.g., Berghuijs et al., 2014; Lins, 1997; Sankarasubramanian et al., 2001). In the eastern part of the country, the total amount of precipitation decreases from east to west and there is no distinct seasonality in precipitation. In the western and central United States, precipitation varies seasonally (higher in winter/lower in summer and lower in winter/higher in summer, respectively). Streamflow regimes are influenced by snowmelt and snow accumulation in the colder northern and high-altitude regions, whereas in the warmer south, atmospheric demand plays a larger role. Besides these natural influences, human influences can also potentially alter the streamflow regime. Over the entire United States, there are many dams and reservoirs that change streamflow properties (Graf, 1999; Lehner et al., 2011). Other human influences that affect these streamflow properties include surface and groundwater abstractions (e.g., Castle et al., 2014), diversions, effluent return flow, hydro-power production, and trans-basin water transfers (Emanuel et al., 2015). There are also various regulations and management practices (e.g., related to environmental or drought response plans) that aim to improve the streamflow conditions, both in the long-term and during drought events.

Meteorological data were sourced from the PRISM data set (PRISM Climate Group, Oregon State University, http://prism.oregonstate.edu). Gridded daily maximum, minimum, and mean temperature (respectively, T_{max}, T_{min}, and T_{mean} [°C]) and precipitation (P [L/T]) were obtained (4 km spatial resolution), for the period 1981–2009. Catchments from the contiguous United States were selected from the Gages-II data set (Falcone, 2011) where streamflow records were required to have continuous daily data between 1981 and 2009. Daily streamflow records for selected catchments were downloaded from the USGS website (https://waterdata.usgs.gov/). As daily PRISM data are available from 1981 and the Hydro-Climatic Data Network 2009 data (HCDN-2009; Lins, 2012) are evaluated up to 2009, the period of analysis was constrained to the period 1981–2009. The spatial distribution of catchments is presented in Figure 1a. Each catchment was labeled as either near-natural (n = 511) or potentially influenced (n = 2067), according to the classification from HCDN-2009.

Impacts of drought are defined by the U.S. Drought Impact Reporter (DIR, http://droughtreporter.unl.edu/map/) as "an observable loss or change that occurred at a specific place and time because of drought." Such drought impacts may be documented, for example, by the media or in scientific or governmental reports. The DIR was initiated by the National Drought Mitigation Centre (NDMC) in July 2005 with the purpose of archiving reported drought impacts (Wilhite et al., 2007). Drought impact reports can be submitted by the general public and are collected in near real time via an online media clipping service. They are then manually moderated, summarized, and sorted into different drought impact categories (e.g., *Agriculture* or *Energy*), and together with their spatial (e.g., county or state) and temporal (start, end, and reporting date) information are stored in the impact database (DIR). For this study, drought impact reports from 2005 to 2009 reported at the county-level were extracted from the DIR together with their categorical classification along with their spatial (i.e., county or counties of impact occurrence) and temporal (start date of reported drought impact) information.

3. Methods

3.1. Drought Index Calculation

Three meteorological drought indices were derived for each catchment: the SPI, the SPEI, and the SMRI. The SPI is based solely on precipitation. The SPEI is based on the difference between precipitation and potential evapotranspiration, where potential evapotranspiration was estimated following the Hargreaves approach (Allen et al., 1998). The SMRI is based on the sum of precipitation and snowmelt minus snow accumulation. Snow accumulation, expressed as the amount of liquid water accumulated as snow, occurs when T_{mean} is smaller than a threshold temperature of 1 °C, whereas snowmelt, expressed as the amount of liquid water melted, was calculated with a simple temperature index model using a melt factor of 3 mm · °C^{-1} · day^{-1} (similar to Freudiger et al., 2014). The different meteorological fluxes were first calculated or derived for each grid cell (partially or wholly) within the catchment (exemplified for one catchment in Figure 1b) and each daily time step between 1981 and 2009, and then aggregated over the catchment. The aggregated daily fluxes were then accumulated over different accumulation periods (n) ranging between $n = 1$ to $n = 12$ months. These aggregated and accumulated fluxes were transformed to their Weibull plotting positions, which were then transformed to the standard normal distribution (a transformation commonly done for these standardized meteorological drought indices) using the approximation described in Abramowitz and Stegun (1964) to derive SPI_n, $SPEI_n$, and $SMRI_n$.

For the calculation of streamflow percentiles, daily streamflow was first aggregated to monthly average time series. Months with regularly occurring zero flow (>25%) were excluded (percentage of excluded months ranges between 0.7% [March] and 2.7% [Septmber]) because it is unhelpful to study streamflow drought (expressed as an anomaly) under these arid conditions where zero flow reflects normal conditions (e.g., Barker et al., 2016). The remaining monthly streamflow records for each catchment and calendar month were transformed to streamflow percentiles (Q_P) using their Weibull plotting positions. Similar to the meteorological drought indices, streamflow percentiles indicate anomalies for a particular month, e.g., streamflow percentiles for January indicate whether January was relatively wet (high values) or dry (low values).

3.2. Link Between Meteorology and Streamflow

For each catchment ($j = 1, 2, \ldots, 2578$) and calendar month ($m = 1, 2, \ldots, 12$), yearly time series of monthly streamflow percentiles $Q_{P,j,m}$ (reflecting the entire flow regime) were correlated with yearly time series of $SPI_{n,j,m}$, $SPEI_{n,j,m}$, and $SMRI_{n,j,m}$ records (also reflecting both wet and dry meteorological anomalies) using Spearman's rank correlation (ρ). From the 36 calculated correlations for each calendar month (three indices with 12 accumulation periods), three metrics were selected, namely:

- $\rho_{max,j,m}$: the maximum correlation found,
- $S_{max,j,m}$: the type of drought index (SPI, SPEI, or SMRI) with the maximum correlation, and
- $A_{max,j,m}$: the corresponding accumulation period of S_{max}.

For ease of notation, the month and catchment identifiers (j and m) are omitted from the variable subscripts in the remainder of this article. Note that S_{max} can be multiple drought indices ($S_{max} > 1$), for example, if ranks of two types of meteorological drought indices are tied, which is often the case for short accumulation periods of the SPI and SMRI during the summer.

3.2.1. Link With Climate Zones

The suitability of the meteorological drought indices and associated accumulation periods to reflect streamflow in catchments with near-natural flow is expected to vary over the different hydro-climatic regions of the United States. To test this, each catchment was classified according to (variations of) two climate classification systems: one that reflects the aridity of a catchment and one that reflects the seasonality in precipitation.

The aridity of the catchment was reflected by the de Martonne Aridity index (A_I, de Martonne, 1926; equation (1))

$$A_I = \frac{P_A}{T_A + 10}, \tag{1}$$

where T_A is the annual average temperature (°C) and P_A the annual average precipitation (mm/year) of the catchment. The seasonality in precipitation was reflected by the precipitation-seasonality component of the Köppen-Geiger climate classification (*K*, modified from the seasonality formulation of Kottek et al., 2006; equation (2));

$$K = \begin{cases} s \text{ if } P_{\text{min,sum}} < 40 \text{ and } P_{\text{min,sum}} < P_{\text{min,win}} \text{ and } P_{\text{max,win}} > 3P_{\text{min,sum}} \\ w \text{ if } P_{\text{min,win}} < 40 \text{ and } P_{\text{min,win}} < P_{\text{min,sum}} \text{ and } P_{\text{max,sum}} > 3P_{\text{min,win}} \\ f \qquad \text{otherwise} \end{cases}. \tag{2}$$

where *s* indicates that summers are drier than winters (87 catchments with near-natural flow), *w* that winters are drier than summers (101 catchments with near-natural flow), and *f* indicates the absence of seasonality in precipitation (323 catchments with near-natural flow). $P_{\text{min,sum}}$ ($P_{\text{min,win}}$) is the minimum average monthly precipitation of the summer (winter) months, and $P_{\text{max,sum}}$ ($P_{\text{max,win}}$) is the maximum average precipitation of the summer (winter) months. Note that in order to make the classification scheme more applicable in the United States, the formulation of the dry winter climate used in this study deviates from the formulation of dry winter climates in Kottek et al. (2006). Where *K* is based on a predetermined classification scheme, A_I is continuous. Catchments with near-natural flow were divided over two A_I groups with $A_I < 50$ (223 catchments) and $A_I \geq 50$ (288 catchments). This distinction is subjective and serves an illustrative purpose; it only separates between relatively drier (not necessarily arid) and wetter (not necessarily very humid) catchments. Catchment locations and classifications according to both A_I and *K* are presented in Figure S3.

3.2.2. Link With Human Influences

Meteorological drought indices are expected to have a lower correlation with streamflow potentially affected by human influences. To test this, it is necessary to separate the effect of human influences on the correlation strength from other factors affecting the strength of this correlation (such as the underlying data or methodological choices). We used the 5th percentile of ρ_{max} of the near-natural streamflow records (ρ_5) as a threshold. Lower correlations are likely a result of various human influences, whereas for higher correlations, it is less certain whether ρ_{max} is lower than one because of human influences or because of an imperfect relationship between meteorological and streamflow drought indices. A more extensive discussion on this as well as the sensitivity to the used ρ_{max}-threshold is presented in the Supplementary Material (S1). We categorize ρ_{max} for each catchment with potentially influenced flow and calendar month as follows:

- *comparable* when ρ_{max} of a potentially influenced streamflow record is above the ρ_{max}-threshold, that is, higher than the 5th percentile of ρ_{max} for catchments with near-natural flow ($\rho_{max} > \rho_5$),
- *weaker* when ρ_{max} of a potentially influenced streamflow record is below the ρ_{max}-threshold but still significant ($\rho_{sig} \leq \rho_{max} < \rho_5$), or
- *non-significant* when ρ_{max} of a potentially influenced streamflow record is non-significant ($\rho_{max} < \rho_{sig}$),

where ρ_{sig} is the significance level of Spearman's rank correlation (here, $\rho_{sig} \geq 0.38$ for $p < 0.05$).

3.3. Link With Locally Reported Drought Impacts

Text-based drought impact data obtained from the DIR were processed as follows. First, impacts categorized by the DIR as *Relief, Response, and Restrictions* were removed because their occurrence is mutually dependent on management decisions and deficits in precipitation or streamflow. The spatial distribution of the remaining

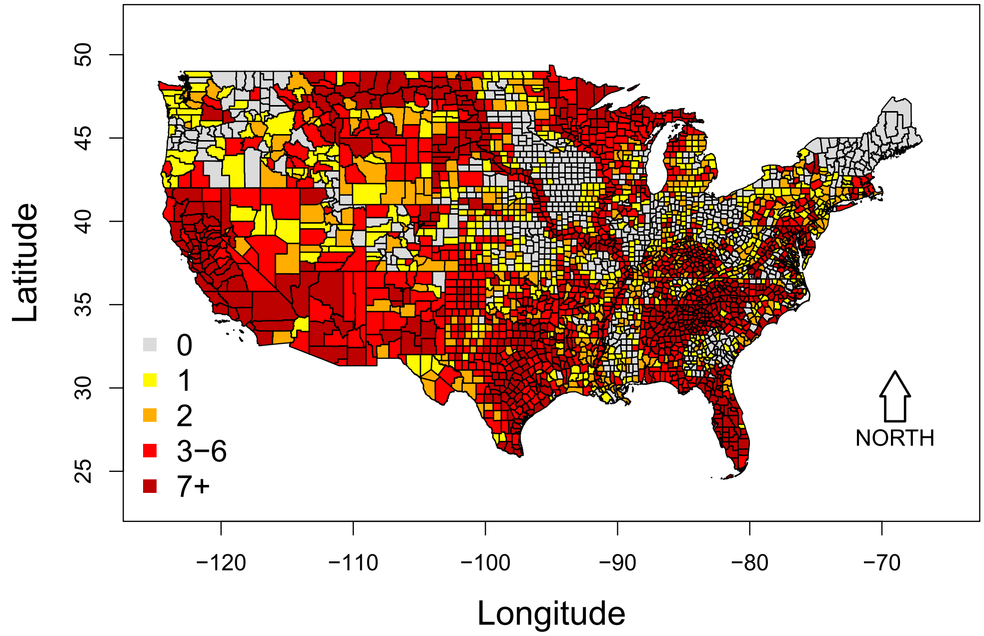

Figure 2. Number of considered reported drought impacts per county archived by the U.S. Drought Impact Reporter from 2005 to 2009.

number of reported drought impact occurrences per county between 2005 and 2009 is shown in Figure 2. The total number of impact occurrences in all counties is 13,308. The total number of impact occurrences per county varies from 0 to 105 (25th percentile = 0, median = 2, 75th percentile = 5). These impacts were then transformed to binary time series of impact occurrence/no impact occurrence for each county at a monthly time step between 2005 and 2009. Counties were intersected with gauging station locations so each streamflow percentile record was linked to a corresponding binary time series of impact occurrence (when multiple gauges were located in a county, they were assigned the same county impact occurrence record). Streamflow percentile values of the month with reported drought impacts in the county of the gauging station location were graphically compared for catchments with near-natural flow and catchments with potentially influenced flow (which were further subdivided for each calendar month according to the correlation categories defined in section 3.2.2, that is, comparable, weaker, and non-significant).

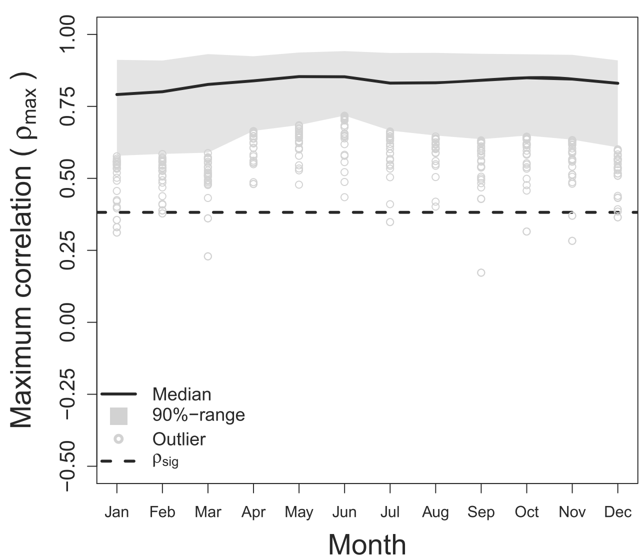

Figure 3. Maximum correlation (ρ_{max}) between streamflow percentiles and three meteorological drought indices (SPI_n, $SPEI_n$, and $SMRI_n$) of different accumulation periods (*n* = 1–12 months) for catchments with near-natural flow for each calendar month.

4. Results

4.1. Link With Climate Zones

For the catchments with near-natural flow (*n* = 511), which serve as a natural reference of the investigated links, Figure 3 shows the maximum correlation (ρ_{max}) between meteorological drought indices (SPI_n, $SPEI_n$, and $SMRI_n$) and streamflow percentiles for each calendar month. In general, there is good agreement between climate and streamflow for these catchments; the median of ρ_{max} varies between 0.79 and 0.85 over the calendar months, with upper bounds of the 90% range of ρ_{max} between 0.91 and 0.94, and lower bounds of the 90% range of ρ_{max} between 0.58 and 0.72. For catchments with near-natural flow, highest correlations are generally found throughout the country depending on the season, for example, California in winter or the northeastern United States in summer (Figure 4a). Lower correlations are generally observed in and east of the Rocky Mountains region in winter and spring and in the southern United States in summer and autumn.

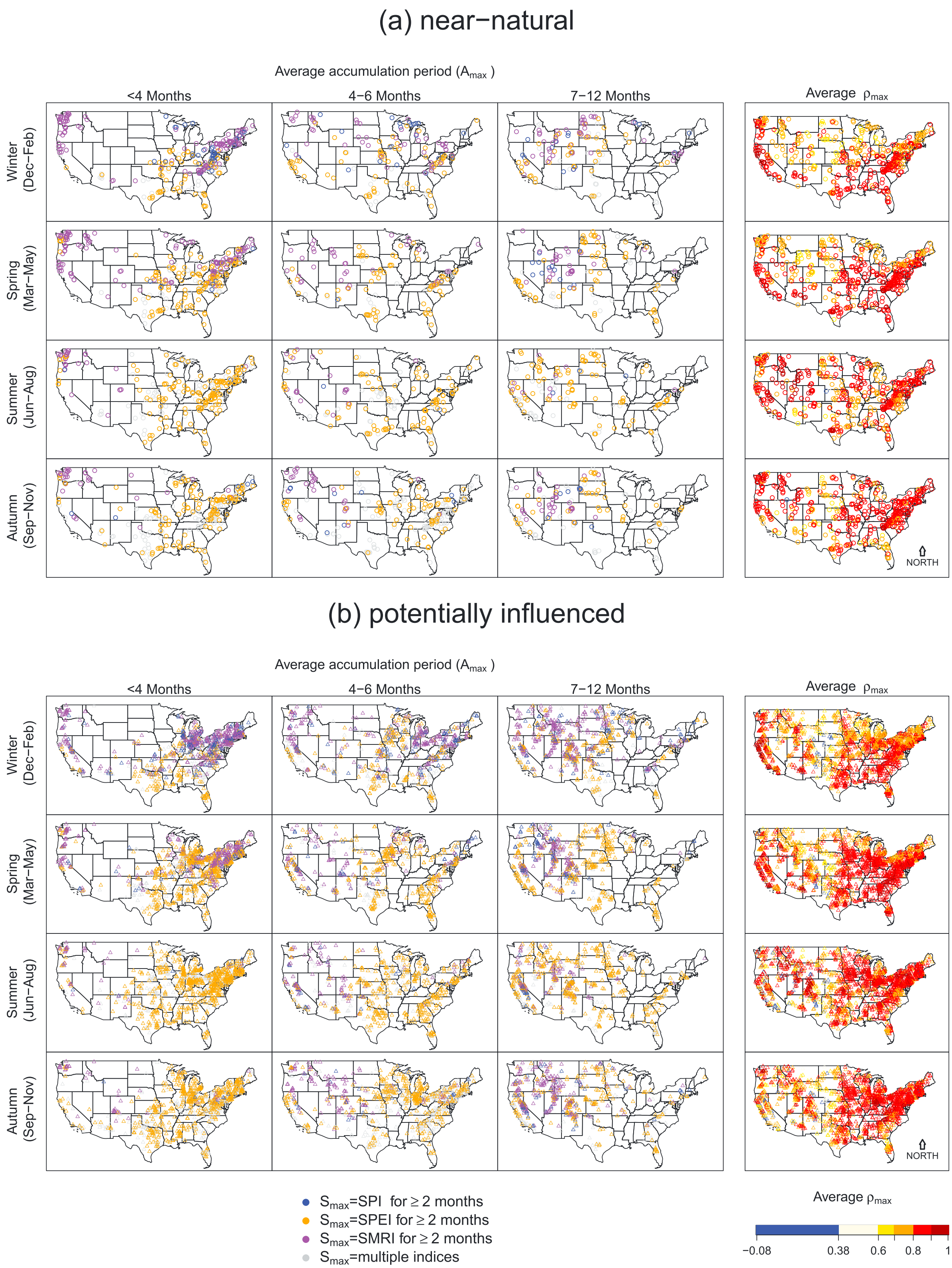

Figure 4. Spatial distribution of the type meteorological drought index (SPI, SPEI, and SMRI) that is most strongly correlated with streamflow percentiles (S_{max}) for at least two out of three calendar months (first three columns) and the average maximum correlation strength (ρ_{max}) (fourth column) in a specific season for catchments with (a) near-natural flow and (b) potentially influenced flow. Rows: seasons; first three columns: separation by ranges of average accumulation period with the strongest correlation (A_{max}) in a specific season. The gray symbols show gauging station locations where S_{max} is not a single drought index for at least two out of three calendar months in the given season.

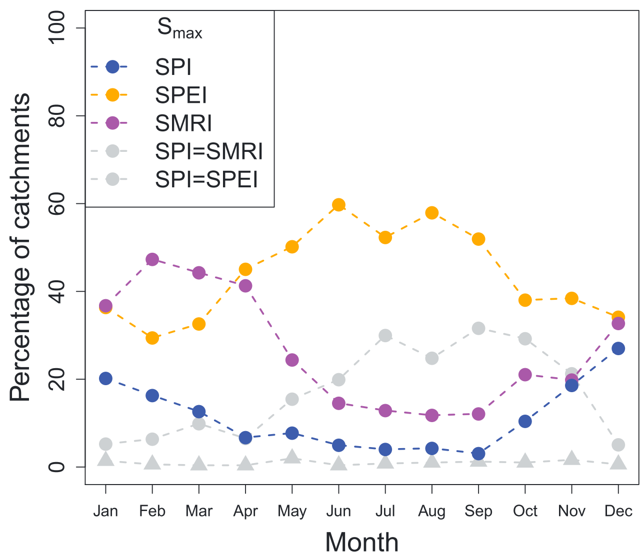

Figure 5. Type of meteorological drought index that is most strongly correlated with streamflow percentiles (S_{max}) for catchments with near-natural flow (expressed as the percentage of catchments) for each calendar month.

Figures 4a and 5 reveal which meteorological drought index has the strongest correlation with streamflow percentiles (S_{max}) for different calendar months and regions across the United States. For most catchments and calendar months, the SPI is not the index with the highest correlation. The percentage of catchments for which S_{max} = SPI varies between calendar months and is highest in winter (up to 27% in December), especially for catchments located in and around the state of Virginia (Figure 4a). The low percentage of catchments for which S_{max} = SPI in summer months is partially related to the regular occurrence of S_{max} = SPI=SPEI (Figure 5; SPI is equal to the SMRI when there is no snowmelt or snow accumulation). At a maximum, S_{max} = SPI and S_{max} = SPI=SMRI account for 35% of the catchments in the summer months (May–September). The SPEI, which takes into account potential evapotranspiration, shows the maximum correlation for a large proportion of catchments in these summer months (50–60% between May and September), especially in the eastern part of the contiguous United States and in California (Figure 4a). The percentage of catchments with S_{max} = SPEI is lower (29–36%) in the winter and early spring months (December–March) and is at a minimum in February (Figure 5). In this winter and (early) spring period, using the SMRI which considers snowmelt and snow accumulation results in higher ρ_{max} for a large proportion of catchments (S_{max} = SMRI for 33–47% of the catchments, especially those catchments located at higher latitudes or in mountainous areas; Figure 4a). However, even in summer months, S_{max} = SMRI for 10–15% (Figure 5), particularly for some catchments located in the Pacific Northwest and Rocky Mountains region (Figure 4a).

The type of meteorological drought index that has the strongest correlation with streamflow percentiles (S_{max}) depends on the region's climatic regime and hence, the geographic location (Figures 4a and 6). For the drier subset of catchments ($A_I < 50$; Figure 6a), especially those located in the southeastern United States (Figure 4a), a relatively large percentage of catchments (39–64%) show S_{max} = SPEI for all calendar months. The percentage of catchments for which S_{max} = SPEI is lowest in February when SMRI peaks (S_{max} = SMRI for 36% of catchments). Snow accumulation and snowmelt play a larger role in the colder (more humid) climates ($A_I \geq 50$). Figure 6b shows a large percentage of catchments with S_{max} = SMRI for winter and spring months (January–April, between 49 and 63% percent of the catchments, mainly located in the higher

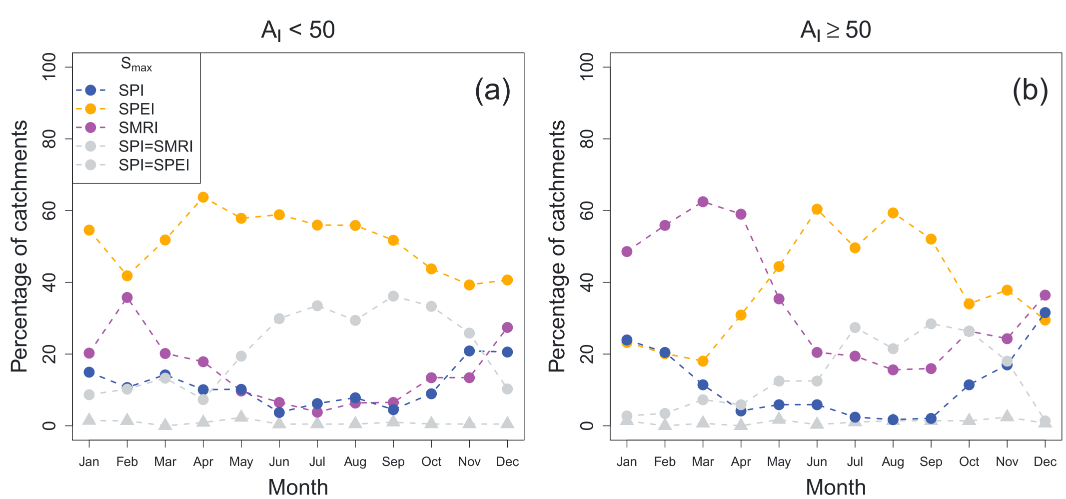

Figure 6. Type of meteorological drought index that is most strongly correlated with streamflow percentiles (S_{max}) for catchments with near-natural flow expressed as the percentage of catchments for the subset of (a) drier and (b) wetter catchments for each calendar month.

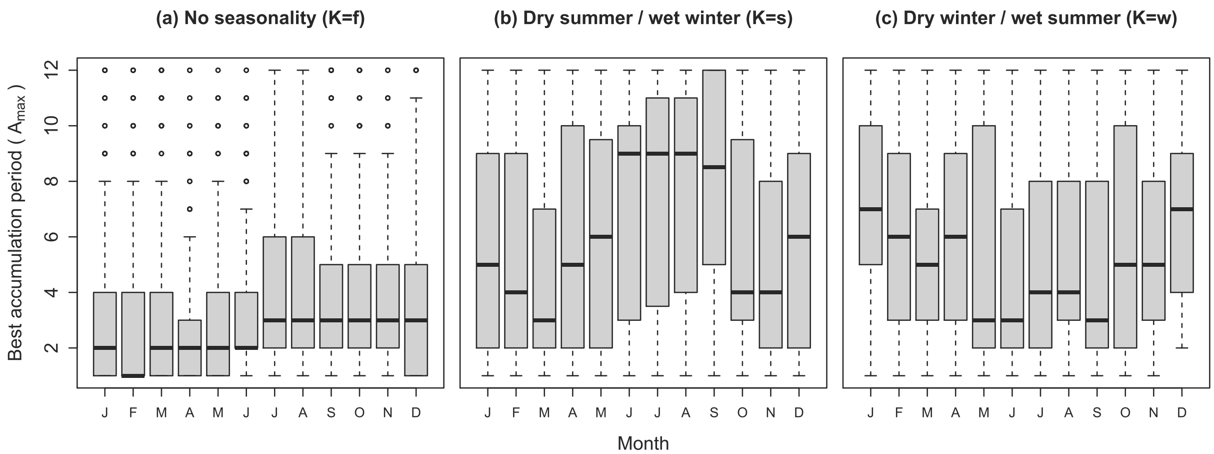

Figure 7. Distribution of the accumulation period of the meteorological drought index that is most strongly correlated with streamflow percentiles (A_{max}) for different calendar months and catchments with near-natural flow. Samples grouped into three Köppen-Geiger (K) classes (equation (2), map in Figure S3); (a) no seasonality in precipitation ($K = f$), (b) seasonality in precipitation (dry summers/wet winters, $K = s$), and (c) seasonality in precipitation (dry winters/wet summers, $K = w$). Box: percentiles 25, 50, and 75. End of whiskers: percentiles 5 and 95. Points: outliers.

latitude regions in the north as well as the more mountainous regions in the west; Figure 4a). However, even for these wetter catchments, S_{max} = SPEI for around 45–60% of the catchments in the summer months (May–September Figure 6b), particularly for catchments located in the northeastern part of the United States (Figure 4a).

In light of these general differences in maximum correlation strength and type of meteorological drought index with the strongest correlation, the question is then how the accumulation period of the meteorological drought index that is most strongly correlated with streamflow percentiles (A_{max}) depends on the climatic setting and hence the location within the United States (Figures 4a and 7). The subgroup of catchments in climates without seasonality in precipitation ($K = f$; Figure S3a) located in the eastern United States and in the Rocky Mountains and the Cascades in the western United States shows no visible temporal pattern in the accumulation period with the strongest correlation with monthly streamflow percentiles (A_{max}; Figure 7a). The median of A_{max} for this group is relatively constant for the different calendar months and varies between 1 and 3. The average standard deviation of A_{max} of the 12 calendar months ($\overline{sd}$) for each catchment in this class is 1.88. For the subgroup of catchments in climates with dry summers and wet winters, mostly the western United States (West Coast, Sierra Nevada, and high plains) ($K = s$; Figure S3a), A_{max} varies more among calendar months and a temporal pattern is visible. A_{max} (both median and 25th and 75th percentiles) is generally shorter in the wetter winter months and longer in the drier summer months (Figure 7b), especially toward the end of the dry season (median between eight and nine months in June–September). The average variation in A_{max} across the calendar months is also higher for catchments in this subgroup having a seasonality signal in precipitation ($\overline{sd} = 2.84$). The opposite pattern is observed for catchments in climate regimes having dry winters and wet summers ($K = w$; Figure S3a), as found in the east part of the Mid-Continent region and the west part of the Midwest region. In this region, A_{max} is shorter in summer (median between three to four months) and longer in winter (median up to seven months) (Figure 7c). The average variation in A_{max} over the year for each catchment is again higher than this variation for climates without seasonality ($\overline{sd} = 2.62$).

4.2. Link With Human Influences

In summary, the maximum Spearman rank correlation (ρ_{max}) of the meteorological drought indices and streamflow percentiles for the sample of streamflow records that are potentially altered by human influences (n = 2067) shows similarities and differences to the values found for the sample of near-natural records (Figures 4b and 8). For the majority of potentially influenced records, there is good agreement between streamflow and meteorological anomalies, with the median (95th percentile) of ρ_{max} varying between 0.78 and 0.86 (0.91 and 0.94) across the calendar months (Figure 8). For the subset of potentially influenced records that have a comparable ρ_{max}, the type of meteorological drought index and accumulation period

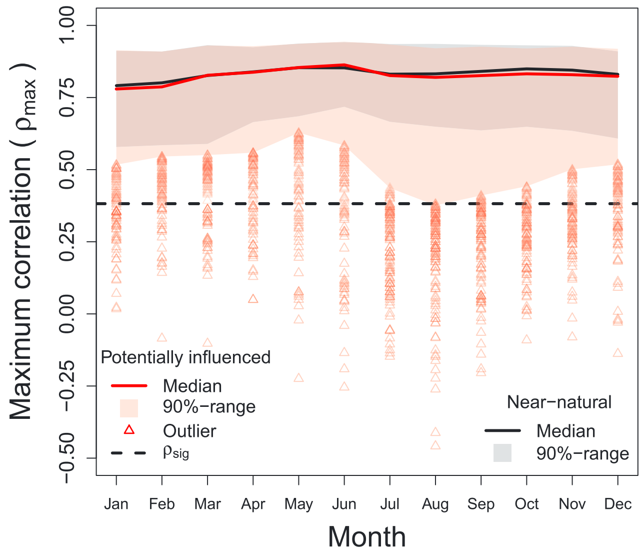

Figure 8. Maximum correlation (ρ_{max}) between three different meteorological drought indices (SPI$_n$, SPEI$_n$, and SMRI$_n$) accumulated over 12 different accumulation periods (n = 1–12 months) and streamflow percentiles (ρ_{max}) for catchments with potentially influenced streamflow records for each calendar month. The median and 90% range of catchments with near-natural flow (Figure 3) are shown for reference.

that has the strongest correlation with streamflow percentiles for different calendar months follows similar patterns as those found for catchments with near-natural flow (Figures S4–S6).

However, not all catchments with potentially influenced streamflow records have correlations comparable to those of catchments with near-natural flow; the 5th percentile of ρ_{max} of potentially influenced flows is notably lower, especially in the month July–October (Figure 8). Where the 5th percentile of ρ_{max} of catchments with near-natural flow varies between 0.58 and 0.72 for different calendar months, the 5th percentile of ρ_{max} of catchments with potentially influenced streamflow records varies between 0.38 and 0.63 and is consistently lower. Notably lower correlations are found, for example, for some catchments in and around Western Nebraska and Eastern Colorado in winter and spring (Figure 4b). In summer, lower correlations are found in California and around. In addition, individual catchments across the United States were also found to have notably lower correlations then their surrounding catchments.

For the majority of potentially influenced records and calendar months, ρ_{max} is classified as comparable to ρ_{max} of near-natural catchments (Figure 9a). The percentage of catchments with ρ_{max} classified as weaker (using the 5th percentile of ρ_{max} for each calendar month as a threshold) varies between 6% (March) and 15% (August). There is a lower percentage of catchments with ρ_{max} classified as weaker in winter and a higher percentage of catchments with ρ_{max} classified as weaker in summer. The percentage of catchments with potentially influenced streamflow records with a non-significant ρ_{max} shows a similar pattern: lower in winter (minimum in February of only 1% of catchments) and higher in summer (maximum in August with 5% of catchments). The spatial distribution of the records that have at least one month classified with ρ_{max} weaker or non-significant is displayed in Figure 9b. Of the catchments that have at least one month with ρ_{max} classified as weaker, a relatively large proportion are located in the western and central United States. Clusters of catchments with at least one month where ρ_{max} is classified as non-significant are mainly visible throughout the western United States, in particular, the West Coast and southwestern United States, although smaller groups are also found in, e.g., the south-northeastern United States. For these catchments with a weaker or non-significant correlation, the temporal pattern of the type of meteorological drought index and

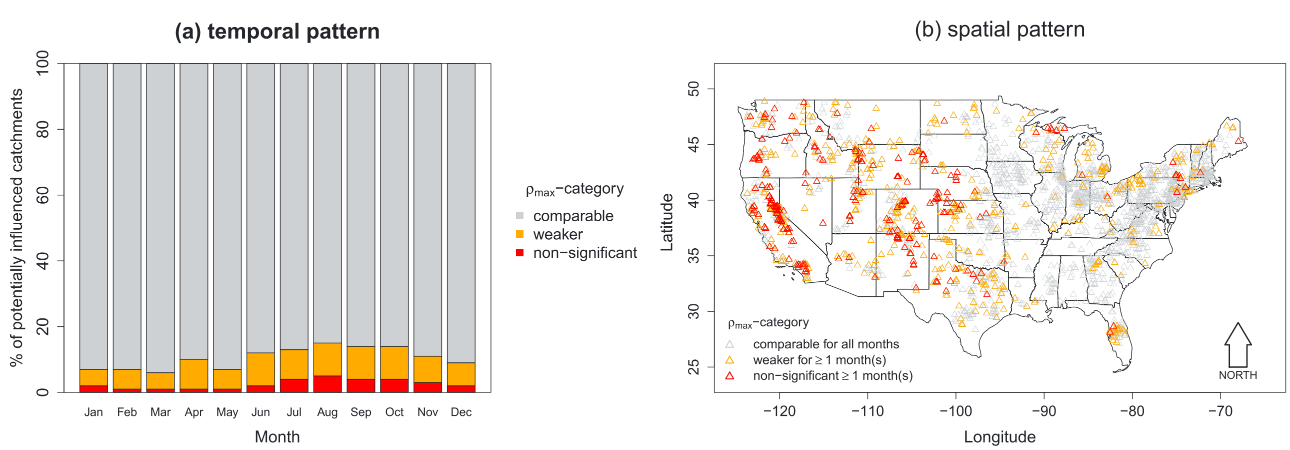

Figure 9. (a) Percentage of potentially influenced catchments with the categorized maximum correlation between streamflow percentiles and three different meteorological drought indices (SPI$_n$, SPEI$_n$, and SMRI$_n$) accumulated over 12 different accumulation periods (n = 1–12 months) for different calendar months; see section 3.2.2. (b) Locations of gauging stations with at least one month of the monthly maximum correlation between meteorological drought indices and streamflow percentiles in the respective correlation categories. Similar graphics for different ρ_{max} thresholds are presented in Figure S1.

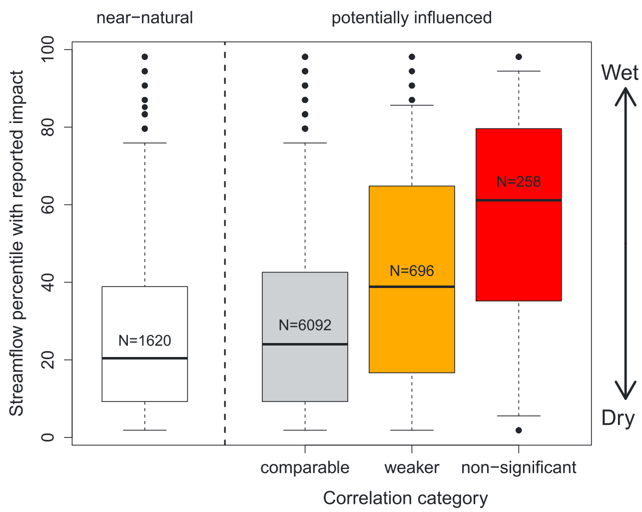

Figure 10. Streamflow percentile values for months with at least one drought impact report in the county of the gauging station location, classified by degree of alteration in maximum correlation (described in section 3.2) using ρ_5 and the non-significance level as threshold. *N* are the number of joint occurrences of available streamflow record(s) in the county of a reported drought impact. Box: percentiles 25, 50, and 75. End of whiskers: percentiles 5 and 95. Points: outliers.

accumulation period that has the maximum correlation with streamflow also differs from those patterns found for catchments with near-natural flow, i.e., the pattern is less distinct or even absent (Figures S4–S6).

4.3. Link With Reported Drought Impacts

Streamflow percentile values were generally low when at least one drought impact was reported in the county of the gauging station, although there was considerable variabilty in the percetiles recorded (Figure 10). There are systematic differences for catchments with near-natural flow, as well as for catchments with potentially influenced flow from the three groups with different maximum correlations between meteorological drought indices and streamflow percentiles. For each group, drought impacts were reported over the entire range of streamflow percentiles (from driest to wettest). For catchments with near-natural flow, 50% of the drought impacts occurred with streamflow percentiles $\leq Q_{21}$ and 75% of impacts with streamflow percentiles $\leq Q_{39}$. These numbers are slightly higher for catchments, and calendar months for which ρ_{max} was classified as comparable (median = Q_{25}, 75th percentile = Q_{43}). However, the number of catchments in the comparable category, and consequently, the number of cases with both a reported drought impact and a streamflow percentile record in the county of the reported drought impact (see section 3.3), was notably higher. Four times as many joint occurrences of streamflow record(s) in a county of a reported drought impact were found for the potentially influenced records compared to the records with near-natural flow. The percentiles with reported drought impacts increase for catchments and calendar months with a correlation category classified as weaker. Half of the impacts occurred with streamflow percentiles $\leq Q_{39}$ and 75% of the impacts occurred with streamflow percentiles $\leq Q_{64}$. Percentile values are even higher for catchments and months with a correlation category classified as non-significant; 50% of the impacts were reported with streamflow percentiles $\leq Q_{61}$ and 75% of the impacts were reported with streamflow percentiles $\leq Q_{79}$. For the latter category, more than 50% of the reported impacts occurred in the wetter range of the streamflow percentiles ($>Q_{50}$).

The geographic distribution of average impact-corresponding streamflow percentiles reveals that in most regions between 2005 and 2009, drought impacts have occurred at below normal streamflow percentiles in most regions (Figure 11). In states such as North Carolina or Texas, streamflow percentiles generally indicated below normal anomalies in months with reported drought impacts (average of Q_P in months with

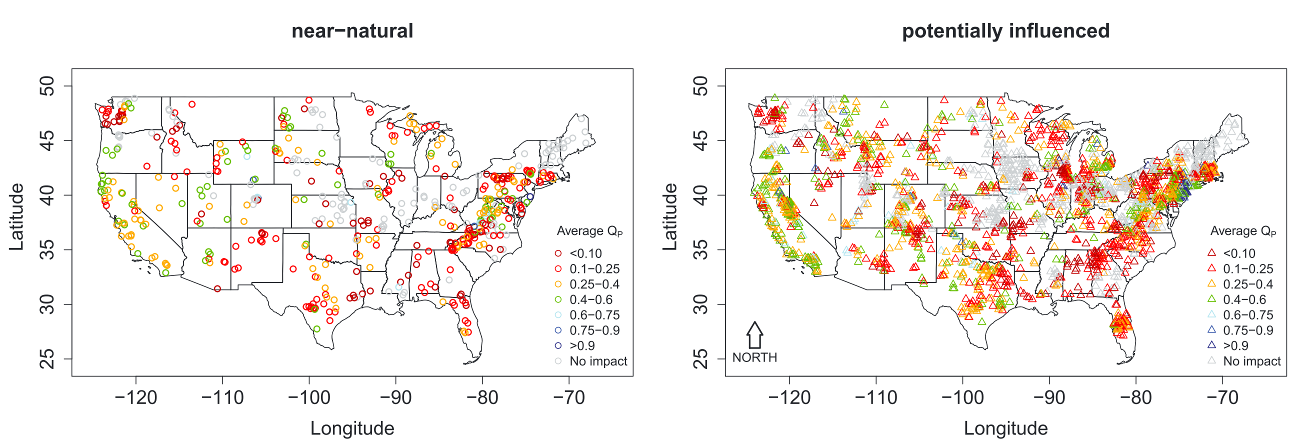

Figure 11. Average streamflow percentile values of months that had at least one reported drought impact in the county of the gauging station between 2005 and 2009, derived for catchments with (a) near-natural flow and (b) potentially influenced flow. The gray symbols are gauging-station locations in counties without drought impact reports between 2005 and 2009.

reported drought impacts $<Q_{25}$). However, for some regions, drought impacts have occurred at higher streamflow percentiles. For example, in California, on average relatively normal conditions (average of $Q_P > Q_{25}$) were found in months with reported drought impacts, both for catchments with near-natural and potentially influenced flow. In some counties, drought impacts were reported in months where streamflow percentile values on average indicated relatively wet condition (average of $Q_P > Q_{75}$), for example, in part of New Jersey and some other counties scattered around the United States.

5. Discussion

5.1. Link With Climate Zones

Although the SPI is most often used in large-scale drought monitoring and early warning systems (Bachmair, Stahl, et al., 2016), it does not appear to have the strongest correlation with streamflow, which is one of the domains of the hydrological cycle where part of the actual impacts of droughts are experienced (Van Lanen et al., 2016). In this study, the SPEI showed a higher maximum correlation with streamflow for a large proportion of the catchments, especially in the summer months and in the drier regions (Figures 4–6). Stronger correlations of the SPEI were also found in other studies for drier regions such as the southwestern United States (McEvoy et al., 2012) and Spain (Vicente-Serrano et al., 2012). Furthermore, streamflow percentiles and the SMRI show stronger correlations, especially in the winter and spring months and in the colder climates (Figures 4–6), which is comparable to patterns found for some (alpine) catchments in Switzerland (Staudinger et al., 2014). The SMRI performs well in the western United States (Figure 4), where the importance of snow accumulation during winter for water availability in the summer is reflected by the use of the Surface Water Supply Index for drought monitoring and early warning (Shafer & Dezman, 1982). The accumulation period of the meteorological drought index with the highest correlation with streamflow percentiles revealed a general pattern related to precipitation seasonality (Figure 7); this best accumulation period varied with the calendar month with shorter accumulation periods for the wet part of the year and longer periods for the dry part of the year. Similar differences in accumulation period with the strongest correlation over the wet and dry season were found for other rivers with seasonal climates, such as the Logone River in central Africa (Nkiaka et al., 2017) or various rivers across the western United States (Abatzoglou et al., 2014; McEvoy et al., 2012). This difference in the observational data confirms the importance of initial conditions at the end of the wet season for streamflow in the dry season found in the model-based study by Van Loon et al. (2014).

Besides the SPI, SPEI, and SMRI, there are a variety of other meteorological drought indices that could have been considered in this study, including the Palmer Drought Severity Index (PDSI; Palmer, 1965); a drought index with great heritage, particularly in the United States. However, although the PDSI is derived with the same meteorological input, its calculation is substantially different to that of the standardized indicators used here and the PDSI was therefore not included in this study. For example, as the PDSI is based on a soil water balance model, it requires additional information on the water holding capacity of soils in the catchment. In addition, the PDSI is not scalable nor is the PDSI comparable over space or time (Alley, 1984). The comparability of the standardized indicators and their relative ease of calculation are attractive qualities in the design and operation of a drought monitoring and early warning system; so much so, that the SPI is recommended by the World Meteorological Society for monitoring meteorological drought (Hayes et al., 2011). The selected meteorological drought indices could have been calculated over more accumulation periods (here they were constrained to 12 months). However, better correlations may have been obtained in some regions of the United States if longer accumulation periods were used, as is shown in, for example, McEvoy et al. (2012) for the southwestern United States (although improvements in correlation were small compared to the correlation obtained with a 12-month accumulation period).

The stronger correlation between streamflow percentiles and the SPEI and SMRI compared to the SPI is promising especially considering the potential further improvements that can be gained with the better representation of potential evapotranspiration/snowmelt and accumulation. For this large-scale assessment, we used the Hargreaves equation to calculate potential evapotranspiration because it only requires precipitation and temperature (mean, minimum, and maximum) as inputs, whereas other potential (or actual) evapotranspiration estimation methods, such as Penman-Monteith, may be more accurate, although they require more input data making them challenging to apply for an operational monitoring and early warning system. Other assumptions were made with regard to the SMRI; the melt factor was fixed to 3 mm · $°C^{-1}$ · day^{-1}, whereas various studies show different optimal melt factors for different locations (e.g., Hock, 2003). A more accurate representation of the magnitude and timing of snowmelt might improve the daily representation of snowmelt and thus the correlation between streamflow and SMRI. Future research could aim to improve the methodological choices, however; the stronger correlations between streamflow percentiles and the SPEI and SMRI (compared to the SPI) achieved with the pragmatic approach used in this study are encouraging for potential applications in the context of large-scale operational drought monitoring systems, which may have operational computational and data constraints.

5.2. Link With Human Influences

A strong link was found between meteorological drought indices and streamflow percentiles for the majority of the catchments with near-natural flow (Figure 3). In addition, comparable strong correlations were found for the majority of the catchments with potentially influenced streamflow (Figure 8). These correlations were mostly comparable, even though there were some differences between the two groups of catchments (i.e., those with near-natural flow and those with potentially influenced flow); for example, catchments with near-natural flow were more likely to be smaller headwater catchments located in areas with lower population densities or economic activities. However, a proportion of potentially influenced records (6–15%; Figure 9a) showed weaker maximum correlations than those found for catchments with near-natural flow using ρ_5 as threshold. The largest proportion of weaker correlations was observed in the summer months (Figure 9a), which agrees with the lower summer correlations found on the Iberian Peninsula by Vicente-Serrano et al. (2014) and the expected higher impacts of human activities on streamflow in these summer months. The percentage of catchments with weaker correlations found in this study is relatively low compared to the percentages found for changes in flow magnitude characteristics in other studies in the United States, for example, the 86% of the catchments studied by Carlisle et al. (2011).

Given that the United States is among the most flow-regulated regions of the world (Lehner et al., 2011), it was surprising that only 6–15% of the catchments show a lower maximum correlation. One reason is the low correlation-threshold used to detect human induced changes in maximum correlation. Increasing this threshold from ρ_5 to ρ_{25} increases the percentage to around 30% of the catchments (depending on the calendar month) but also increases the uncertainty whether a lower ρ_{max} is caused by human influences or not (see supporting information S1). Other reasons might be related to the variety of ways human influences can modify the streamflow (drought) signal. The use of rank correlation was particularly suitable for this study as it directly compares meteorological and hydrological anomalies, which form that basis of many drought monitoring and early warning products that mostly use anomaly information (and not absolute values) to display the drought situation. However, a high maximum correlation does not imply that the streamflow (drought) record is free of human influences. The strongest effect on the correlation occurs when human influences counteract the natural situation, for example, compensation flows during meteorological drought and flood control (holding back water in the reservoir) during high meteorological anomalies (exemplified in Figure 12b). More subtle changes in correlation can be a result of human induced trends or step changes (exemplified in Figures 12c and 12d). Strong trends or step changes can diminish the correlation greatly; however, weak trends or step changes only have a small impact on the correlation and the diminished correlation caused by these weak trends or step changes could very well fall within the range of uncertainty defined for catchments with near-natural flow. There are also human influences that only affect flow magnitude, for example, in the case of constant and systematic abstractions (Figure 12e) or in the case that abstractions vary as a function of the degree of dryness (Figure 12f). These changes in monthly flow magnitude do not mean a change in the ranking of monthly flow and do not affect the correlation. Different studies investigate the absolute and temporal changes in mean, minimum, or maximum flow and relate these changes to various human activities (e.g., Carlisle et al., 2011; Rice et al., 2015, 2016; Sadri et al., 2016). Future research could aim to modify these approaches to identify absolute and temporal changes in drought characteristics, such as drought occurrence, duration, or deficit volume, something which was beyond the scope of the current study. Furthermore, only looking at the maximum correlation between streamflow and the meteorology introduces a bias. For example, streamflow in a responsive catchment with a reservoir might have a weak correlation with a meteorological drought index accumulated over a short-term accumulation period (as would be expected for a responsive natural catchment; Barker et al., 2016) but may have a strong correlation with a meteorological drought index accumulated over a longer period. Additionally, the correlation is based on the entire flow regime (both wet and

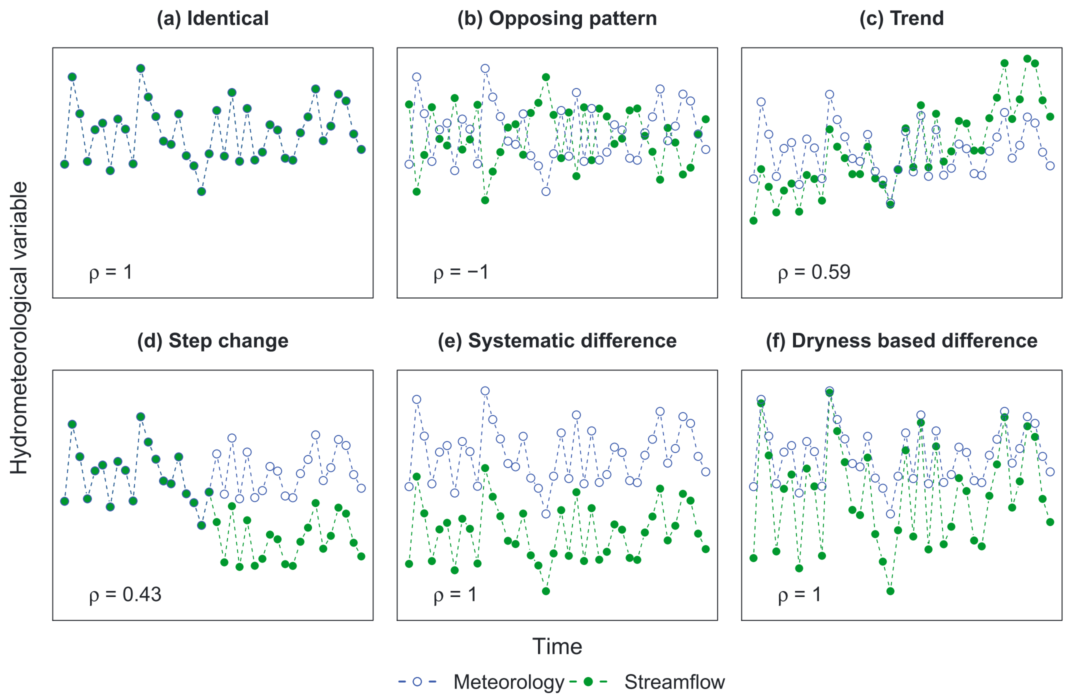

Figure 12. Different types of human induced modifications of the propagating streamflow signal (hypothetical) and corresponding effect on the correlation between streamflow and meteorology. (a) No impact (series are identical), (b) streamflow signal opposes the meteorological signal, (c) trend in the streamflow signal, (d) step change in the streamflow signal, (e) systematic absolute change in the streamflow signal, and (f) absolute change in the streamflow signal as a function of the degree of dryness.

dry years) and a human-induced reduction in correlation between meteorological and streamflow drought indices during dry streamflow anomalies might be concealed by a strong correlation during high flow anomalies.

Clusters of potentially influenced catchments with weaker or non-significant correlations between the meteorological indices and streamflow (Figure 9b) indicate regions where human influences alter the drought response. These spatial clusters correspond to locations where human influences were found to affect streamflow in previous studies, for example, in a comparison between observed and expected (statistically modeled) flow characteristics, Carlisle et al. (2011) found most severe changes in flow magnitude characteristics in the central and western United States. In a modeling experiment, Emanuel et al. (2015) showed that the largest deviations from natural flow conditions related to water transfers occurred in the central and the northeastern United States. For California, He et al. (2017) showed better agreement between observed and modeled streamflow when different human influences (e.g., different reservoir operations, abstractions, and irrigation) were added to the modeling framework. For Florida, Schmidt et al. (2001) suggested that the absence of a relationship between the El Niño–Southern Oscillation (ENSO) and streamflow signals was related to various human influences (such as dams and effluent return from groundwater pumping).

5.3. Link With Reported Drought Impacts

This study is among the first to use DIR information at the scale of the contiguous United States to validate whether streamflow drought hazard indicators also reflect the overall impact occurrence of drought as reported in, e.g., the media. The spatial pattern in the number of reported drought impacts between 2005 and 2009 (Figure 2) matches well with the major drought events in this time frame as archived by the USDM (http://droughtmonitor.unl.edu/Maps/MapArchive.aspx), such as: the 2006 drought in Texas, the 2007–2008 drought in North Carolina, or the 2007–2009 drought in California. However, besides areas with major drought events, the paths of some rivers, such as the Missouri river, can be seen in Figure 2. The occurrence of these river paths can be related to the way some drought impact reports were spatially aggregated; that is, if a particular river is affected, the impact report is sometimes aggregated to all counties this river intersects. Thus, even though impacts are on a county level, they might not always represent the local conditions, eventually leading to a mismatch between larger scale drought impacts for an entire river length and the more local streamflow data of small (headwater) catchments. Another bias is introduced because some drought impacts are observed after the drought event is over. For example, water prices might increase after a drought event because of lost revenue due to water usage restrictions during the drought event. We filtered out most of these impacts by removing relief, response, and restriction impacts; however, some misclassified postevent impact reports may still be among the reported drought impacts. Such postevent impacts are the reason for a mismatch between streamflow drought indicator and reported drought impacts in, for example, New Jersey, where drought impacts occurred at relatively high streamflow percentiles (Figure 11).

Despite the biases described above, drought impacts reported in the DIR mainly occur when streamflow percentile values are low and thus indicate drought conditions (Figures 10 and 11). For the catchments with near-natural streamflow records, or for catchments that have a maximum correlation between meteorological drought indices and streamflow percentiles that is comparable to that of near-natural catchments, 50% of the impacts occurred at or below streamflow percentile values of Q_{21} (catchment with near-natural records) or Q_{25} (catchments with comparable correlations). These percentile values approximate the commonly used monthly variable threshold level for streamflow drought analyses, that is, Q_{20} (e.g., Andreadis et al., 2005; Sheffield et al., 2009) and the Q_{25} percentile threshold level used for the below normal flow category in USGS WaterWatch. These threshold values are also within the range of the median threshold values for the occurrence of drought impacts related to hydrology for some federal states of Germany (Bachmair et al., 2015) and regions of the UK (Bachmair, Svensson, et al., 2016).

Not all potentially influenced streamflow records reflect the reported drought impacts well. For potentially influenced streamflow records classified with a weaker or non-significant maximum correlation with different meteorological drought indices, impact reports occur at higher streamflow percentile levels that do not indicate negative anomalies or drought. The occurrence of impacts at higher percentile values is expected for some of these records, because in case of a weak correlation, the streamflow signal could counteract the meteorological signal (exemplified in Figure 12b); for example, when reservoir outflow is used to compensate for low flow further downstream. In that case, the hazard indicator does not match with the overall drought impact occurrence. Trends and step changes (exemplified in Figures 12c and 12d) could also remove the link between streamflow drought hazard indicators and reported drought impacts. Strong positive trends or step changes (e.g., those caused by the construction of a reservoir in the middle of a record) potentially hinder a streamflow drought index to detect drought conditions. However, overall drought impacts related to other domains of the hydrological cycle might still occur. Strong negative trends or step changes (exemplified in Figure 12d), on the other hand, might cause the streamflow records to continuously indicate negative anomalies. In that case, impacts happen at the expected low streamflow percentiles but the false alarm rate is likely to be higher. From an overall drought monitoring perspective with the aim of mapping the streamflow drought hazard and anomalies, systematic changes (Figures 12e and 12f) are least problematic as percentile time series derived from those streamflow records still indicate the climatic variability and associated drought impacts. However, from a streamflow perspective, the diminished flow might have severe impacts on the instream situation and more research to quantitative relationships is needed for recommendations on streamflow-specific drought management. It is therefore important to emphasize that we only evaluate streamflow records on their capability of reflecting the overall impacts of drought and refrain from any judgment of whether the diminished correlation is good or bad.

5.4. Potential Improvements for Large-Scale Drought Monitoring and Early Warning

For drought monitoring and decision making at the smaller scale (e.g., river basin), local decision makers will have more detailed knowledge about the drought governing processes than what was available in this study. At the larger scale, for example, national to continental (i.e. the focus of this study), such detailed knowledge is often not available and generalizable information such as natural patterns and human-induced deviations from those patterns as presented in this study is extremely useful.

Currently, meteorological (precipitation based) drought indices, such as the SPI, are the most commonly used in (large-scale) drought monitoring and early warning systems (Bachmair, Stahl, et al., 2016*)*. However, Van Lanen et al. (2016) stress the need that hydrological drought information should be considered as well, as it is more closely related to the actual source of the drought impacts. Results of this study confirm the benefit of including streamflow information by showing that the actual drought impacts, as reported by the DIR, often occur at negative streamflow anomalies, for both catchments with near-natural flow and the majority of catchments with potentially influenced streamflow records (Figures 10 and 11). Thus, there is merit in using observed streamflow data in large-scale drought monitoring and early warning applications, and if these data are available and free of large human disturbances, its use should be preferred over the use of meteorological surrogates. However, there are two main limitations with the use of observed streamflow data: (1) it is often not available (in near-real time) for all locations and (2) observed streamflow data are not necessarily free of large human influences, which, according to our results, can cause a mismatch between the streamflow drought hazard indicators and the overall (reported) impacts of drought. In those cases, meteorological drought indices should be used to reflect the hydrological situation. The most suitable meteorological proxy should be chosen instead of using an arbitrary choice of meteorological indicator and accumulation period. Our findings show that the most suitable index is often not the most commonly used SPI, but rather the SPEI or SMRI, and that the best accumulation period also varies, depending on the time of the year, location, and climatic region.

6. Conclusions

Knowledge about the propagation of anomalies from meteorological to streamflow droughts across different climatic regions, and for near-natural and human influenced streamflow records, provides an important basis for large-scale drought monitoring and early warning information. This study of streamflow records across the contiguous United States identified meteorological drought indices that best reflect streamflow anomalies. For a large proportion of catchments with near-natural flow, streamflow was most strongly correlated to the SPEI in the summer months (especially in the drier climates) and to the SMRI in the winter months (especially in the wetter (colder) climates). Furthermore, a general pattern was observed between the accumulation period of the meteorological drought index that has the strongest correlation with streamflow and the time of year for climates with seasonal precipitation regimes. Longer accumulation periods of the standardized indices show stronger correlations in the dry seasons of these seasonal climates, which highlights their dependence on the initial conditions at the start of the dry season. Knowing which meteorological drought index and which accumulation period has the strongest correlation with streamflow in different climatic settings may be used to provide a more impact-targeted large-scale drought monitoring and early warning for ungauged catchments or regions that lack near real-time streamflow data availability.

For catchments where streamflow is potentially altered by human influences, the maximum correlation between meteorological drought indices and streamflow percentiles was found to be largely comparable to those correlations found for catchments with near-natural flow. Although a comparable correlation does not mean that these records are free of other human-induced changes in, for example, flow magnitude, it has important implications for large-scale drought monitoring and early warning of the overall drought situation, which often relies on anomaly information. For catchments with either near-natural flow or with a comparable correlation between meteorological drought indices and streamflow percentiles, drought impacts in the county of the gauging station mainly occurred when streamflow percentiles were low. Streamflow percentiles of these catchments with potentially influenced streamflow records are thus equally suitable for display in a drought information system, for example, to portray the regional drought situation.

However, a subset of about 6–15% of the records of the potentially influenced catchments had a weaker maximum correlation when considering the group with a lower correlation then the 5th percentile of the maximum correlation for catchments with near-natural flow. Most weakened relationships were found in the month of August, that is, in summer, when the impacts of human influences may be most severe. The analysis of reported drought impacts and streamflow percentiles for records and calendar months with a weakened correlation confirms a larger disconnect between meteorological drought indices and streamflow at times of severe drought. For influenced streamflow records with weaker maximum correlations, corresponding drought impacts did not necessarily occur at the expected low streamflow percentiles. Hence, streamflow drought indices derived from these records are less suitable for portraying the overall impacts of drought. This study consequently suggests that knowing when and where correlations between meteorological and hydrological anomalies are weaker due to human influences on flow can help to identify suitable streamflow records for large-scale drought monitoring and early warning information maps.

Acknowledgments

This study is an outcome of the international Belmont Forum/G8HORC's Freshwater Security program project DrIVER (Drought Impacts: Vulnerability thresholds in monitoring and Early warning Research). The authors acknowledge funding toward the DrIVER project from the German Research Foundation DFG (project STA-632/2-1), the UK Natural Environment Research Council (grant NE/L010038/1), and NSF (ICER-1342949). Streamflow data used in this study can be obtained from http://waterdata.usgs.gov/nwis. A list of considered gauging stations used is available upon request. Daily meteorological data (PRISM) used in this study are available at http://www.prism.oregonstate.edu/. Reported drought impacts stem from the U.S. Drought Impact Reporter and are available at http://droughtreporter.unl.edu/map/.

References

Abatzoglou, J. T., Barbero, R., Wolf, J. W., & Holden, Z. A. (2014). Tracking interannual streamflow variability with drought indices in the U.S. Pacific Northwest. *Journal of Hydrometeorology*, *15*(5), 1900–1912. https://doi.org/10.1175/JHM-D-13-0167.1

Abramowitz, M., & Stegun, I. A. (1964). *Handbook of mathematical functions with formulas, graphs, and mathematical tables*. New York: Dover Publications.

Allen, R. G., Pereira, L. S., Raes, D., & Smith, M. (1998). *Crop evapotranspiration - Guidelines for computing crop water requirements, FAO Irrigation and Drainage Paper 56*. Rome: FAO.

Alley, W. M. (1984). The Palmer drought severity index: Limitations and assumptions. *Journal of Climate and Applied Meteorology*, *23*(7), 1100–1109. https://doi.org/10.1175/1520-0450(1984)023<1100:TPDSIL>2.0.CO;2

Andreadis, K. M., Clark, E. A., Wood, A. W., Hamlet, A. F., & Lettenmaier, D. P. (2005). Twentieth-century drought in the conterminous United States. *Journal of Hydrometeorology*, *6*(6), 985–1001. https://doi.org/10.1175/JHM450.1

Bachmair, S., Kohn, I., & Stahl, K. (2015). Exploring the link between drought indicators and impacts. *Natural Hazards and Earth System Sciences*, *15*(6), 1381–1397. https://doi.org/10.5194/nhess-15-1381-2015

Bachmair, S., Stahl, K., Collins, K., Hannaford, J., Acreman, M., Svoboda, M., et al. (2016). Drought indicators revisited: The need for a wider consideration of environment and society. *Wiley Interdisciplinary Reviews: Water*, *3*(4), 516–536. https://doi.org/10.1002/wat2.1154

Bachmair, S., Svensson, C., Hannaford, J., Barker, L. J., & Stahl, K. (2016). A quantitative analysis to objectively appraise drought indicators and model drought impacts. *Hydrology and Earth System Sciences*, *20*(7), 2589–2609. https://doi.org/10.5194/hess-20-2589-2016

Barker, L. J., Hannaford, J., Chiverton, A., & Svensson, C. (2016). From meteorological to hydrological drought using standardised indicators. *Hydrology and Earth System Sciences*, *20*(6), 2483–2505. https://doi.org/10.5194/hess-20-2483-2016

Berghuijs, W. R., Sivapalan, M., Woods, R. A., & Savenije, H. H. G. (2014). Patterns of similarity of seasonal water balances: A window into streamflow variability over a range of time scales. *Water Resources Research*, *50*, 5638–5661. https://doi.org/10.1002/2014WR015692

Carlisle, D. M., Wolock, D. M., & Meador, M. R. (2011). Alteration of streamflow magnitudes and potential ecological consequences: A multiregional assessment. *Frontiers in Ecology and the Environment*, *9*(5), 264–270. https://doi.org/10.1890/100053

Castle, S., Thomas, B., Reager, J., Rodell, M., Swenson, S., & Famiglietti, J. (2014). Groundwater depletion during drought threatens future water security of the Colorado River Basin. *Geophysical Research Letters*, *41*, 5904–5911. https://doi.org/10.1002/2014GL061055

Coopersmith, E., Yaeger, M. A., Ye, S., Cheng, L., & Sivapalan, M. (2012). Exploring the physical controls of regional patterns of flow duration curves – Part 3: A catchment classification system based on regime curve indicators. *Hydrology and Earth System Sciences*, *16*(11), 4467–4482. https://doi.org/10.5194/hess-16-4467-2012

de Martonne, E. (1926). L'indice d'aridité. *Assoc. Geogr*, *3*, 3–5.

Emanuel, R. E., Buckley, J. J., Caldwell, P. V., McNulty, S. G., & Sun, G. (2015). Influence of basin characteristics on the effectiveness and downstream reach of interbasin water transfers: Displacing a problem. *Environmental Research Letters*, *10*(12), 124005. https://doi.org/10.1088/1748-9326/10/12/124005

Falcone, J. A. (2011). *GAGES-II: Geospatial attributes of gages for evaluating streamflow*. Reston: USGS.

Freudiger, D., Kohn, I., Stahl, K., & Weiler, M. (2014). Large-scale analysis of changing frequencies of rain-on-snow events with flood-generation potential. *Hydrology and Earth System Sciences*, *18*, 2695–2709. https://doi.org/10.5194/hess-18-2695-2014

Graf, W. L. (1999). Dam nation: A geographic census of American dams and their large-scale hydrologic impacts. *Water Resources Research*, *35*(4), 1305–1311. https://doi.org/10.1029/1999WR900016

Hannah, D. M., Demuth, S., van Lanen, H. A. J., Looser, U., Prudhomme, C., Rees, G., et al. (2011). Large-scale river flow archives: Importance, current status and future needs. *Hydrological Processes*, *25*(7), 1191–1200. https://doi.org/10.1002/hyp.7794

Haslinger, K., Koffler, D., Schöner, W., & Laaha, G. (2014). Exploring the link between meteorological drought and streamflow: Effects of climate-catchment interaction. *Water Resources Research*, *50*, 2468–2487. https://doi.org/10.1002/2013WR015051

Hayes, M., Svoboda, M., Wall, N., & Widhalm, M. (2011). The Lincoln declaration on drought indices: Universal meteorological drought index recommended. *Bulletin of the American Meteorological Society*, *92*(4), 485–488. https://doi.org/10.1175/2010BAMS3103.1

He, X., Wada, Y., Wanders, N., & Sheffield, J. (2017). Intensification of hydrological drought in California by human water management. *Geophysical Research Letters*, *44*, 1777–1785. https://doi.org/10.1002/2016GL071665

Hock, R. (2003). Temperature index melt modelling in mountain areas. *Journal of Hydrology*, *282*(1–4), 104–115. https://doi.org/10.1016/S0022-1694(03)00257-9

Kottek, M., Grieser, J., Beck, C., Rudolf, B., & Rubel, F. (2006). World map of the Köppen-Geiger climate classification updated. *Meteorologische Zeitschrift*, *15*(3), 259–263. https://doi.org/10.1127/0941-2948/2006/0130

Lehner, B., Liermann, C. R., Revenga, C., Vörömsmarty, C., Fekete, B., Crouzet, P., et al. (2011). High-resolution mapping of the world's reservoirs and dams for sustainable river-flow management. *Frontiers in Ecology and the Environment*, *9*(9), 494–502. https://doi.org/10.1890/100125

Lins, H. F. (1997). Regional streamflow regimes and hydroclimatology. *Water Resources Research*, *33*(7), 1655–1667. https://doi.org/10.1029/97WR00615

Lins, H. F. (2012). *USGS Hydro-Climatic Data Network 2009 (HCDN-2009)*. Reston: USGS.

López-Moreno, J. I., Vicente-Serrano, S. M., Begueria, S., Garcia-Ruiz, J. M., Portela, M. M., & Almeida, A. B. (2009). Dam effects on droughts magnitude and duration in a transboundary basin: The lower river tagus, pain and Portugal. *Water Resources Research*, *45*, W02405. https://doi.org/10.1029/2008WR007198

López-Moreno, J. I., Vicente-Serrano, S. M., Zabalza, J., Beguería, S., Lorenzo-Lacruz, J., Azorin-Molina, C., & Morán-Tejeda, E. (2013). Hydrological response to climate variability at different time scales: A study in the Ebro basin. *Journal of Hydrology*, *477*, 175–188. https://doi.org/10.1016/j.jhydrol.2012.11.028

McEvoy, D. J., Huntington, J. L., Abatzoglou, J. T., & Edwards, L. M. (2012). An evaluation of multiscalar drought indices in Nevada and eastern California. *Earth Interactions*, *16*(18), 1–18. https://doi.org/10.1175/2012EI000447.1

McKee, T. B., Doesken, N. J., & Kleist, J. (1993). The relationship of drought frequency and duration to time scales. Paper Presented at the 8th Conference on Applied Climatology, AMS, Anaheim.

Nkiaka, E., Nawaz, N. R., & Lovett, J. C. (2017). Using standardized indicators to analyse dry/wet conditions and their application for monitoring drought/floods: A study in the Logone catchment, Lake Chad basin. *Hydrological Sciences Journal*, *62*(16), 2720–2736. https://doi.org/10.1080/02626667.2017.1409427

Palmer, W. C. (1965). Meteorological drought. Weather Bur. Res. Pap. 45, U.S. Dep. Of commerce, Washington, US.

Peters, E., Torfs, P. J., Van Lanen, H. A., & Bier, G. (2003). Propagation of drought through groundwater—A new approach using linear reservoirtheory. *Hydrological Processes*, *17*(15), 3023–3040. https://doi.org/10.1002/hyp.1274

Rangecroft, S., Van Loon, A. F., Maureira, H., Verbist, K., & Hannah, D. M. (2016). Multi-method assessment of reservoir effects on hydrological droughts in an arid region. *Earth System Dynamics Discussions*, 1–32. https://doi.org/10.5194/esd-2016-57

Rice, J. S., Emanuel, R. E., & Vose, J. M. (2016). The influence of watershed characteristics on spatial patterns of trends in annual scale streamflow variability in the continental US. *Journal of Hydrology*, *540*, 850–860. https://doi.org/10.1016/j.jhydrol.2016.07.006

Rice, J. S., Emanuel, R. E., Vose, J. M., & Nelson, S. A. (2015). Continental US streamflow trends from 1940 to 2009 and their relationships with watershed spatial characteristics. *Water Resources Research*, *51*, 6262–6275. https://doi.org/10.1002/2014WR016367

Sadri, S., Kam, J., & Sheffield, J. (2016). Nonstationarity of low flows and their timing in the eastern United States. *Hydrology and Earth System Sciences*, *20*(2), 633–649. https://doi.org/10.5194/hess-20-633-2016

Sankarasubramanian, A., Vogel, R. M., & Limbrunner, J. F. (2001). Climate elasticity of streamflow in the United States. *Water Resources Research*, *37*(6), 1771–1781. https://doi.org/10.1029/2000WR900330

Schmidt, N., Lipp, E. K., Rose, J. B., & Luther, M. E. (2001). ENSO influences on seasonal rainfall and river discharge in Florida. *Journal of Climate*, *14*(4), 615–628. https://doi.org/10.1175/1520-0442(2001)014<0615:EIOSRA>2.0.CO;2

Seager, R., Hoerling, M., Schubert, S., Wang, H., Lyon, B., Kumar, A., et al. (2015). Causes of the 2011-14 California drought. *Journal of Climate*, *28*(18), 6997–7024. https://doi.org/10.1175/JCLI-D-14-00860.1

Shafer, B. A., & Dezman, L. E. (1982). Development of a surface water supply index (SWSI) to assess the severity of drought conditions in snowpack runoff areas. *Proceedings of the 50th Annual Western Snow Conference*, *50*, 164–175.

Sheffield, J., Andreadis, K. M., Wood, E. F., & Lettenmaier, D. P. (2009). Global and continental drought in the second half of the twentieth century: Severity-area-duration analysis and temporal variability of large-scale events. *Journal of Climate*, *22*(8), 1962–1981. https://doi.org/10.1175/2008JCLI2722.1

Staudinger, M., Stahl, K., & Seibert, J. (2014). A drought index accounting for snow. *Water Resources Research*, *50*, 7861–7872. https://doi.org/10.1002/2013WR015143

Stoelzle, M., Stahl, K., Morhard, A., & Weiler, M. (2014). Streamflow sensitivity to drought scenarios in catchments with different geology. *Geophysical Research Letters*, *41*, 6174–6183. https://doi.org/10.1002/2014GL061344

Svoboda, M., LeComte, D., Hayes, M., Heim, R., Gleason, K., Angel, J., et al. (2002). The drought monitor. *Bulletin of the American Meteorological Society*, *83*(8), 1181–1190. https://doi.org/10.1175/1520-0477(2002)083<1181:TDM>2.3.CO;2

Tallaksen, L. M., & Van Lanen, H. A. J. (2004). *Hydrological drought, volume 48: Processes and estimation methods for streamflow and groundwater, Development in Water Science* (Vol. 48). Amsterdam: Elsevier Science B.V.

Tijdeman, E., Hannaford, J., & Stahl, K. (2018). Human influences on streamflow drought characteristics in England and Wales. *Hydrology and Earth System Sciences Discussions*, 1–27. https://doi.org/10.5194/hess-2017-430

Van Lanen, H. A. J., Laaha, G., Kingston, D. G., Gauster, T., Ionita, M., Vidal, J. P., et al. (2016). Hydrology needed to manage droughts: The 2015 European case. *Hydrological Processes*, *30*(17), 3097–3104. https://doi.org/10.1002/hyp.10838

Van Lanen, H. A. J., Wanders, N., Tallaksen, L. M., & Van Loon, A. F. (2013). Hydrological drought across the world: Impact of climate and physical catchment structure. *Hydrology and Earth System Sciences*, *17*(5), 1715–1732. https://doi.org/10.5194/hess-17-1715-2013

Van Loon, A. F. (2015). Hydrological drought explained. *Wiley Interdisciplinary Reviews: Water*, *2*(4), 359–392. https://doi.org/10.1002/wat2.1085

Van Loon, A. F., Ploum, S. W., Parajka, J., Fleig, A. K., Garnier, E., Laaha, G., & Van Lanen, H. A. J. (2015). Hydrological drought types in cold climates: Quantitative analysis of causing factors and qualitative survey of impacts. *Hydrology and Earth System Sciences*, *19*(4), 1993–2016. https://doi.org/10.5194/hess-19-1993-2015

Van Loon, A. F., Tijdeman, E., Wanders, N., Van-Lanen, H. A. J., Teuling, A. J., & Uijlenhoet, R. (2014). How climate seasonality modifies drought duration and deficit. *Journal of Geophysical Research: Atmospheres*, *119*, 4640–4656. https://doi.org/10.1002/2013JD020383

Van Loon, A. F., & Van Lanen, H. A. J. (2012). A process-based typology of hydrological drought. *Hydrology and Earth System Sciences*, *16*(7), 1915–1946. https://doi.org/10.5194/hess-16-1915-2012

Van Loon, A. F., & Van Lanen, H. A. J. (2013). Making the distinction between water scarcity and drought using an observation-modeling framework. *Water Resources Research*, *49*, 1483–1502. https://doi.org/10.1002/wrcr.20147

Vicente-Serrano, S. M., Beguería, S., & López-Moreno, J. I. (2010). A multiscalar drought index sensitive to global warming: The standardized precipitation evapotranspiration index. *Journal of Climate*, *23*(7), 1696–1718. https://doi.org/10.1175/2009JCLI2909.1

Vicente-Serrano, S. M., Beguería, S., Lorenzo-Lacruz, J., Camarero, J. J., López-Moreno, J. I., Azorin-Molina, C., et al. (2012). Performance of drought indices for ecological, agricultural, and hydrological applications. *Earth Interactions*, *16*(10), 1–27. https://doi.org/10.1175/2012EI000434.1

Vicente-Serrano, S. M., Lopez-Moreno, J. I., Beguería, S., Lorenzo-Lacruz, J., Sanchez-Lorenzo, A., García-Ruiz, J. M., et al. (2014). Evidence of increasing drought severity caused by temperature rise in southern Europe. *Environmental Research Letters*, *9*(4), 1–9. https://doi.org/10.1088/1748-9326/9/4/044001

Wilhite, D. A., Svoboda, M. D., & Hayes, M. J. (2007). Understanding the complex impacts of drought: A key to enhancing drought mitigation and preparedness. *Water Resources Management*, *21*(5), 763–774. https://doi.org/10.1007/s11269-006-9076-5

Zhang, Y.-K., & Schilling, K. E. (2006). Increasing streamflow and baseflow in Mississippi River since the 1940s: Effect of land use change. *Journal of Hydrology*, *324*(1–4), 412–422. https://doi.org/10.1016/j.jhydrol.2005.09.033